ORIENTATION AND MOTION OF A FLUORESCENT PROBE IN MODEL MEMBRANES*

R.A. Badley, H. Schneider and W.G. Martin

Biochemistry Laboratory,
National Research Council of Canada
Ottawa, Ontario, Canada

Received July 27, 1971

SUMMARY: A method has been developed, based on polarized fluorescence intensity measurements, for studying the orientation and motion of fluorescent probes incorporated into lipid bilayers. Its use is illustrated in a study of the effect of cholesterol in egg lecithin multibilayers. When no cholesterol is present the probes are constrained to angles between 0° and 80° to the normal to the plane and show, superimposed, a rapid but restricted motion. The angular distribution decreases to a limiting range of 0° to 67° as cholesterol is increased to 25-30 mole % but the rapid motion is unaffected.

INTRODUCTION

The use of fluorescence techniques in the study of biological and biologically relevant model systems is now well established (1,2,3). The present paper describes a method for measuring the orientation and motion properties of a fluorescent probe in multibilayer structures. Application to egg lecithin bilayers shows that cholesterol restricts the probes' angular distribution relative to the normal to the plane of the bilayers without changing the fast but restricted movement of their long axes.

---

*N.R.C.C. Publication Number

MATERIALS AND METHODS

Egg lecithin was prepared by chromatography on alumina and silicic acid and stored at -30°C. Cholesterol was recrystallized twice from methanol before use. The fluorescent probe, 2,2'(vinylenedi-p-phenylene)bisbenzoxazole, (VPBO) (Fig. 1) was a generous gift from Dr. G. McGraw of Tennessee Eastman Company. The rigidity of VPBO make it especially useful as a probe for measuring the motions and orientations of long chain molecules such as phospholipids.

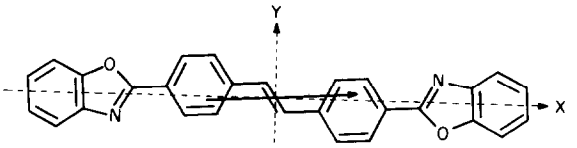

Fig. 1. Structure of VPBO. The arrow indicates the direction of the transition moment.

Uncorrected excitation and fluorescence spectra were recorded on a Farrand spectrofluorimeter. The quantum yield which was insensitive to solvent polarity was determined to be 0.85 by comparing the integrated fluorescence spectrum to that of 2,5-bis(5-tert-butylbenzoxazolyl)(2)thiophene (BBOT) whose quantum yield is 0.74 (4). The fluorescence lifetime of VPBO was calculated by the method of Birks and Dyson (5) and was also measured on a single photon counting apparatus to be approximately 1 nsec.

Egg lecithin multibilayers were prepared on plane surfaces (glass or silica) by slowly drying down, with wet nitrogen, chloroform solutions of the lipids. The films were then kept in vacuo for two hours to remove residual chloroform. Hydration was carried out by exposure for 2-3 hours to nitrogen

saturated with water vapour and then the film was compressed between two plane surfaces (6). Films which had been in contact for 24 hours with water vapour or for 30 mins. with mammalian Ringer's solution gave very similar results. The presence of multibilayers in films prepared in identical fashion was confirmed by X-ray diffraction (7). The polarized fluorescence intensities were measured using a specially designed fluorimeter in which the configuration of detector, light source and sample can easily be varied.

THEORY OF THE FLUORESCENCE EXPERIMENT AND RESULTS

The fourth moments of the orientation distribution function of a fluorescent probe incorporated into an ordered structure can be determined from polarized fluorescence intensities. As shown by Desper and Kimura (8) all the intensity information is contained in a matrix or grid of nine intensity values, I_{ij} (i,j = 1-3), obtained by taking the nine different

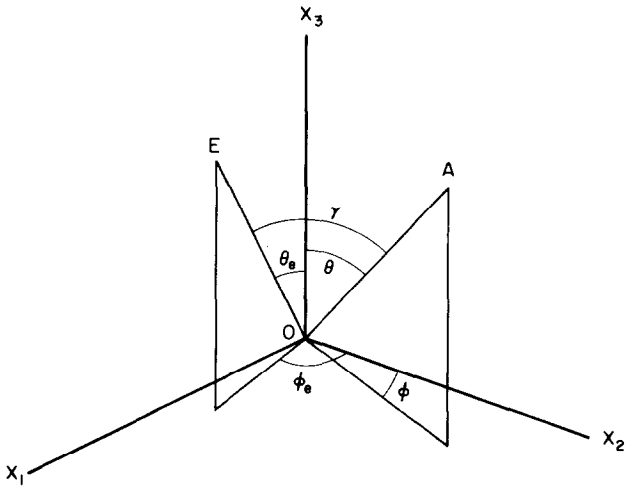

Fig. 2. Diagram of the cartesian coordinate system ($OX_1X_2X_3$) used to define the angles $\theta, \theta_e, \gamma, \phi$ and ϕ_e. OA and OE represent the absorption and emission vectors respectively.

combinations of excitation (i) and emission (j) polarization directions parallel to the i and j axes of a Cartesian coordinate system, $X_1X_2X_3$ (Fig. 2) which is itself fixed in the sample. The matrix is

$$I = \begin{vmatrix} I_{11} & I_{12} & I_{13} \\ I_{21} & I_{22} & I_{23} \\ I_{31} & I_{32} & I_{33} \end{vmatrix}$$

Analysis of the case where a non-mobile fluorescent probe has a single fixed linear oscillator along which both absorption and emission vectors lie has been carried out by Desper and Kimura (8). Biaxial symmetry (the X_1X_2, X_1X_3 and X_2X_3 planes are mirror planes of symmetry for the distribution function) or uniaxial symmetry (cylindrical symmetry around a preferred axis) was assumed.

The present study extends the treatment of Desper and Kimura for uniaxial models to situations where the conditions $I_{22}/I_{21} = 3$ and $I_{ij} = I_{ji}$ $(i \neq j)$ may fail. Both fail if the absorption and emission oscillators are non-parallel, if resonance energy transfer occurs between non-parallel probes or if the probe undergoes a rotational diffusion of rate comparable to the fluorescence decay. For these three cases each oscillator was considered to have moved through a fixed angle γ, during the fluorescence lifetime. However, if the rotational diffusion of the oscillator is fast compared to the lifetime but the extent of motion is limited, the absorption and emission oscillators are randomized within the defined solid angle, i.e. γ can take any value between 0 and the physical limit of the motion, γ_{max}. In such a case $I_{22}/I_{21}<3$ but $I_{ij} = I_{ji}$ $(i \neq j)$. That non-parallelism of absorption and emission vectors and energy transfer were not responsible for the observed decrease of I_{22}/I_{21} from 3 for the lecithin films was confirmed by determining I_{22}/I_{21} for a dilute

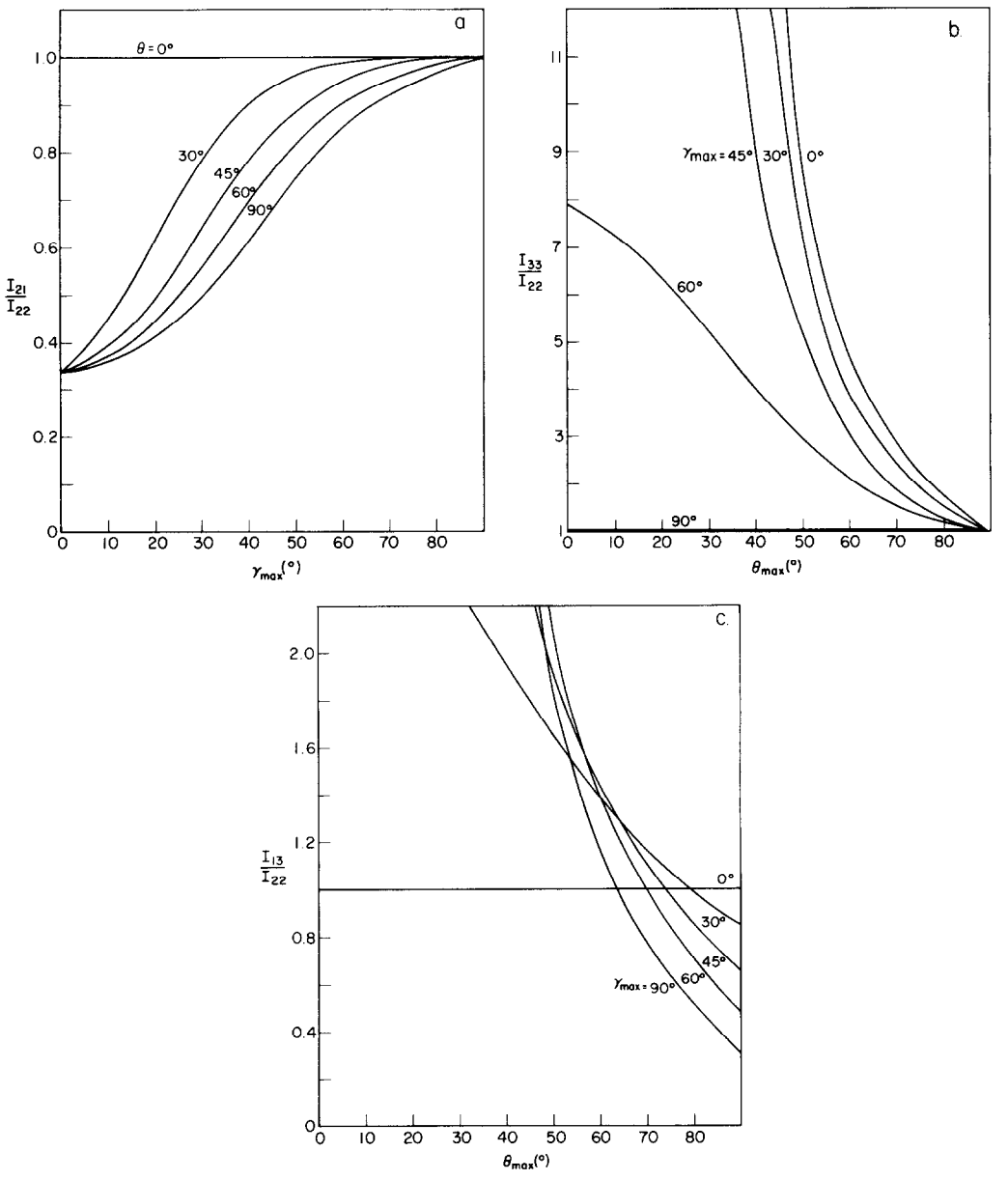

Fig. 3. Calculated I_{ij}/I_{22} values for model 1. (a), I_{21}/I_{22} against γ_{max} for values of θ_{max}. (b), I_{33}/I_{22} against θ_{max} for values of γ_{max}. (c), I_{13}/I_{22} against θ_{max} for values of γ_{max}.

(a) Ordinate , I_{21}/I_{22}
Abscissa , γ_{max}
(b) Ordinate , I_{33}/I_{22}
Abscissa , θ_{max}
(c) Ordinate , I_{13}/I_{22}
Abscissa , θ_{max}

viscous solution of VPBO and by diluting it in the films.

In general, the fluorescence matrix is as given in Table 1 where the brackets denote average values over the distribution of θ, θ_e, ϕ and ϕ_e (Fig. 2). Axial symmetry around X_3 was assumed and confirmed by examination of the films under a polarizing microscope. The mathematical models calculated are summarized in Table 2. Model 1 was found to fit best the present system and is shown graphically in Fig. 3 from which appropriate matrices can be constructed. Symmetry conditions show these calculations are applicable to the complete three dimensional array of probes.

Table 1

Expressions for I_{ij} derived from Fig. 2

$$= \begin{vmatrix} \langle \sin^2\theta \sin^2\phi \sin^2\theta_e \sin^2\phi_e \rangle & \langle \sin^2\theta \sin^2\phi \sin^2\theta_e \cos^2\phi_e \rangle & \langle \sin^2\theta \sin^2\phi \cos^2\theta_e \rangle \\ \langle \sin^2\theta \cos^2\phi \sin^2\theta_e \sin^2\phi_e \rangle & \langle \sin^2\theta \cos^2\phi \sin^2\theta_e \cos^2\phi_e \rangle & \langle \sin^2\theta \cos^2\phi \cos^2\theta_e \rangle \\ \langle \cos^2\theta \sin^2\theta_e \sin^2\phi_e \rangle & \langle \cos^2\theta \sin^2\theta_e \cos^2\phi_e \rangle & \langle \cos^2\theta \cos^2\theta_e \rangle \end{vmatrix}$$

Table 2

Summary of models used in calculations of fluorescence matrices. θ_{max} and γ_{max} were varied between 0° and 90°.

Model	θ	γ
1	Distributed from 0° to θ_{max}	Distributed from 0° to γ_{max}
2	Same fixed angle for all probes	Distributed from 0° to γ_{max}
3	Distributed from 0° to θ_{max}	Same fixed angle for all probes
4	Same fixed angle for all probes	Same fixed angle for all probes

Although the calculations lead to matrices whose sum is unity it has been found advantageous to measure the intensities in the form I_{ij}/I_{22} and therefore the results are presented in this form. At low values of θ and γ it is not easy to distinguish between models 1 and 2 but at such angles (<20°) physical differences between the two cases are becoming small.

The corrected excitation and fluorescence spectra of VPBO in an egg lecithin multibilayer film are shown in Fig. 4.

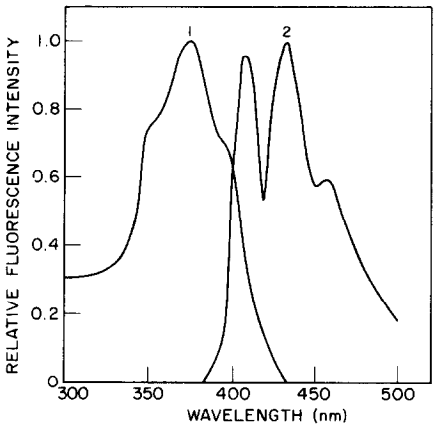

Fig. 4. Corrected excitation (1) and fluorescence (2) spectra of VPBO in an egg lecithin film.

Ordinate, Relative fluorescence intensity
Abscissa, Wavelength (nm)

The matrices (I_{ij}/I_{22}) for the egg lecithin films containing 0.02 mole % of VPBO and varying concentrations of cholesterol (0-50 mole %) are given in Table 3 together with the angles θ_{max} and γ_{max} derived for them. Fluorescence excitation was at 380 nm and the emission was isolated by Wratten filters (2C + 2E).

DISCUSSION

Because of its extremely hydrophobic nature VPBO is probably located in the central region of the bilayer. The data indicate that the long axes of the probes are randomly distributed

Table 3

Fluorescence matrices for egg lecithin multibilayers containing 0-50 mole % cholesterol. The relative accuracy of θ_{max} and γ_{max} has been estimated as ±3°.

Mole % Cholesterol	Matrix	θ_{max}	γ_{max}
0	1.0 0.50 0.55 0.50 1.0 0.55 0.55 0.55 1.5	80°	30°
10	1.0 0.50 0.70 0.50 1.0 0.70 0.70 0.70 1.6	79°	30°
20	1.0 0.50 0.85 0.50 1.0 0.85 0.85 0.85 1.8	75°	29°
30	1.0 0.50 0.90 0.50 1.0 0.90 0.90 0.90 2.8	67°	28°
40	1.0 0.50 1.1 0.50 1.0 1.1 1.1 1.1 3.0	67°	28°
50	1.0 0.50 1.1 0.50 1.0 1.1 1.1 1.1 3.0	67°	28°

with a range of θ values rather than having a fixed value, since model 1 provides a better fit than model 2. The large range of θ may represent a motion of the probe which is slow on the nanosecond time scale of the fluorescence experiment, rather than a rigid array. This slow motion, which would require a relaxation time >10 nsec. would reflect, by implication, a feature of the lipid chains. There are superimposed on the distribution of the probes' long axes, rapid motions, of relaxation time <1 nsec., of the type described in the previous section, with a restricted

angular range of 0° to 30°. These are indicated by the values of I_{21}/I_{22} and I_{13}/I_{31}. The fast motion may reflect rapid motion of the lipid chains about their average positions during the nanosecond sampling time. However, the rapid motion may also be due in part to the existence of holes or free space within the bilayer interior, either present naturally or caused by the probes. This latter possibility must be considered because the dimensions of probe and lipid chains are comparable.

The effect of cholesterol is to restrict the angular range of distribution of the probe (θ_{max} decreases) without altering its rapid motion. The change in θ_{max} is equivalent to a 25% reduction in available volume (solid angle). That 25-30 mole % cholesterol saturates the observed fluorescence changes correlates well with similar saturating effects observed by several criteria (9-11) and implies a common underlying structural cause.

The motional and orientational information provided by the fluorescence method, NMR (12) and spin labels (9) can differ because the various probes and techniques may sample different regions of the bilayer and employ different time scales. Since a definitive description of molecular events will obviously require data obtained using a variety of techniques, the fluorescence method described provides a useful tool for understanding the molecular factors controlling membrane structure and function.

ACKNOWLEDGEMENTS

Dr. F.R. Lipsett is thanked for the use of his lifetime apparatus and Dr. A.W. Hanson for examining samples by X-ray diffraction.

REFERENCES

1. Waggoner, A.S. and Stryer, L. Proc. Nat. Acad. Sci. (Wash.), 67, 579 (1970).
2. Yguerabide, J. and Stryer, L. Abs. Biophys. Soc. Meeting New Orleans, Feb. 1971.
3. Badley, R.A. and Teale, F.W.J. J. Mol. Biol. 44, 71 (1969).
4. Berlman, I.B. Handbook of Fluorescence Spectra of Aromatic Molecules. Academic Press, London and New York, (1965).
5. Birks, J.B. and Dyson, D.J. Proc. Royal Soc. (Ser. A) 275, 135 (1963).
6. Seelig, J. J. Am. Chem. Soc. 92, 3881 (1970).
7. Levine, Y.K. and Wilkins, M.H.F. Nature (New Biol.), 230, 69 (1971).
8. Desper, C.R. and Kimura, I. J. Appl. Phys. 38, 4225 (1967).
9. Hsia, J.-C., Schneider, H. and Smith, I.C.P. Can. J. Biochem. 49, 614 (1971).
10. Shah, D.O. and Schulman, J.H. J. Lipid Res. 8, 215 (1967).
11. Lecuyer, H. and Derivichian, D.G. J. Mol. Biol. 45, 39 (1969).
12. Chapman, D. and Penkett, S.A.P. Nature, 211, 1304 (1966).